

Molecular orientation in thin films of bis(1,2,5-thiadiazolo)-*p*-quinobis(1,3-dithiole) on graphite studied by angle-resolved photoelectron spectroscopy

Shinji Hasegawa, Shoji Tanaka, Yoshiro Yamashita, and Hiroo Inokuchi
Institute for Molecular Science, Myodaiji, Okazaki 444, Japan

Hitoshi Fujimoto

Department of Environmental Science, The Graduate School of Science and Technology, Kumamoto University, Kumamoto 860, Japan

Koji Kamiya and Kazuhiko Seki

Department of Chemistry, Faculty of Science, Nagoya University, Nagoya 464-01, Japan

Nobuo Ueno

Department of Materials Science, Faculty of Engineering, Chiba University, Inage-ku Chiba 263, Japan

(Received 14 December 1992)

Angle-resolved ultraviolet photoelectron spectra using synchrotron radiation were measured for oriented thin films of bis(1,2,5-thiadiazolo)-*p*-quinobis(1,3-dithiole) on a cleaved highly oriented pyrolytic graphite (HOPG) surface. The observed takeoff angle dependence of the photoelectron intensity was analyzed by using the independent-atomic-center approximation and modified neglect of diatomic overlap molecular-orbital calculations. The calculated results agree well with the experimental ones. From the comparison between these results, the molecules in the thin film are estimated to lie flat with the inclination angle $\beta \leq 10^\circ$ to the HOPG surface. This analysis method is useful as a first step to a quantitative analysis for angular distribution of photoelectrons from thin films of large and complex organic molecules.

INTRODUCTION

Angle-resolved ultraviolet photoelectron spectroscopy (ARUPS) with use of synchrotron radiation is a powerful method for studying the orientation of molecules in thin films and adsorbates on surfaces.^{1,2} Rigorous theoretical models for angle-resolved photoemission from adsorbates on surfaces were presented previously.³⁻⁵ They took account of various final-state effects of photoelectrons, and showed excellent agreement with experimental results on adsorbed small molecules such as CO and N₂.^{6,7} However, these theories do not allow easy analyses of experimental results for large organic molecules. Since it is important in the field of molecular devices to determine the orientations of functional organic molecules in their thin films and at surfaces, a simple and reasonable method of analysis for large organic molecules is highly desirable.

Several ARUPS experiments on large organic molecules with various theoretical models have been reported.⁸⁻¹⁵ Netzer and Ramsey *et al.* studied the molecular orientation of C₂N₂, benzene, pyridine, and diphenyl on a Pd(110) surface.^{8,9} Yannoulis, Frank, and Koch carried out experiments on anthracene and tetracene on Ag(111) and Cu(100) surfaces.^{10,11} In their works, they determined the molecular orientation with the aid of other methods such as NEXAFS (near-edge x-ray-absorption fine structure) and LEED (low-energy electron diffraction), and the experimental results of ARUPS were only qualitatively analyzed by simple symmetry considerations. In an earlier work, Permien *et al.* measured

ARUPS spectra of lead phthalocyanine thin films on a Cu(100) surface. They deduced a flat-lying orientation of the molecules by comparing the observed angular distribution of photoelectrons with calculated ones.¹² In their calculation, they approximated the molecular orbital by a single p_z atomic orbital and used a plane-wave final state. The use of a plane-wave final state is inadequate, as commented by Richardson.¹³ Richardson recalculated the angular distribution using the spherical-harmonics expansions for final states, and found better agreement with the experimental results by Permien *et al.* This theoretical method was also used in analyzing the experimental results of adsorbed benzene on a Pd(100) surface by Nyberg and Richardson,¹⁴ and pyridine on a Cu(110) surface by Bandy, Lloyd, and Richardson.⁵ In all these approaches a molecule was approximated by a single-point emitter. The approximation is too simplified to apply to large and complex organic molecules. Actually, these methods are insufficient to explain our ARUPS results for oriented thin films of bis(1,2,5-thiadiazolo)-*p*-quinobis(1,3-dithiole) (BTQBT).

BTQBT (Fig. 1) has an extended π -electron system composed of C, N, and S. It shows remarkably low resistivity for a single-component organic system.¹⁶ The resistivity of a single crystal grown by recrystallization is $1.2 \times 10^3 \Omega \text{ cm}$, and it also shows a Hall effect which is rarely observable in organic semiconductors.¹⁷ BTQBT molecules in a single crystal have strong intermolecular interactions, as in the case of other single-component semiconductors.¹⁸ They form a two-dimensional net-

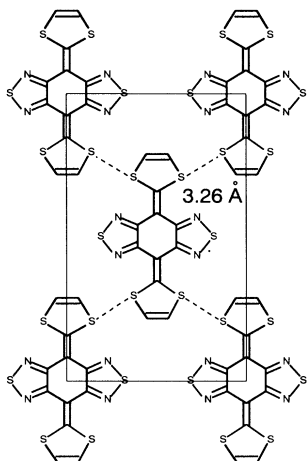


FIG. 1. The sheetlike structure of the two-dimensional network in the BTQBT single-crystal (Ref. 16). The distance of the $S \cdots S$ contact (3.26 Å) is much shorter than the van der Waals radii (3.40 Å).

work between neighboring molecules by short $S \cdots S$ contact (3.26 Å), as shown in Fig. 1. In the network sheet, each molecule is inclined by about 5° to the sheet along the long molecular axis.¹⁶

We measured ARUPS spectra of BTQBT thin films on a highly oriented pyrolytic graphite (HOPG) surface using synchrotron radiation. For a quantitative analysis of the takeoff angle (θ) dependence of photoelectrons from the next-highest and highest occupied molecular-orbital (NHOMO and HOMO) bands, we used the independent-atomic-center (IAC) approximation^{19,20} combined with MNDO (modified neglect of diatomic overlap) molecular-orbital calculations.²¹ In this method, a molecule is regarded as a set of independent atomic emitters, and the single-scattering effect by each atomic hole potential is considered. Although the method neglects other final-state effects,³⁻⁵ it provides almost similar results to those obtained from more rigorous multiple-scattering formalism⁶ in the case of small molecular adsorbates such as carbon monoxide.²⁰ For large organic molecules, however, no comparison between the experimental and theoretical results has even been carried out. In this paper, we report the comparative study using this analysis method on large organic molecules such as BTQBT. The calculated angular distributions of photoelectrons agree well with the experimental results, and a molecular orientation in the thin films is estimated.

EXPERIMENT

The experiments were carried out at the UVSOR Facility (beamline 8B2) in the Institute for Molecular Science.²² The synchrotron radiation was monochromatized by a plane-grating monochromator.²³ The incidence photon energy was $h\nu=40$ eV and the total-energy resolution of the spectra was 0.15 eV. The incidence beam was focused to a size of ≈ 1 mm². The takeoff angle (θ) dependence of the photoemission intensity was measured at incidence angle of photons $\alpha=0^\circ$,

where the detector was placed within the polarization plane of the synchrotron radiation. The angular resolution at the measurements was about 2° .

BTQBT was synthesized as reported,¹⁶ and purified by repeated sublimation. It was carefully evaporated on HOPG substrate (Union Carbide ZYA grade), cleaved in a vacuum of $\approx 10^{-10}$ Torr. The pressure during evaporation was $\approx 10^{-8}$ Torr and the deposition rate was 0.2 Å/min. The substrate was kept at room temperature during the film deposition. The film thickness was estimated with a quartz thickness monitor to be about 30 Å. The sample was then transferred to the measurement chamber ($\approx 4 \times 10^{-10}$ Torr) under vacuum for *in situ* ARUPS measurements.

RESULTS AND DISCUSSION

In Fig. 2, the θ dependence of ARUPS spectra on the BTQBT thin film is shown in the binding-energy region of 0~3.5 eV. The two peaks *A* and *B* are well separated from other valence bands, and assigned by Fujimoto *et al.* to be b_{3g} (NHOMO) and b_{1u} (HOMO) π molecular orbitals, respectively, in D_{2h} symmetry.²⁴ The contribution of photoelectrons from the substrate was negligible, since the film is thicker than the effective escape depth (≤ 10 Å) of photoelectrons, and no characteristic structure due to HOPG was observed in this energy region. With the increase in θ , the intensities of both bands *A* and *B* in Fig. 2 first increase, exhibit a maximum, and decrease subsequently. Following significant differences are observed for these bands: (1) the intensity of the NHOMO band exhibits a maximum at $\theta_{\max} \approx 37.5^\circ$, while

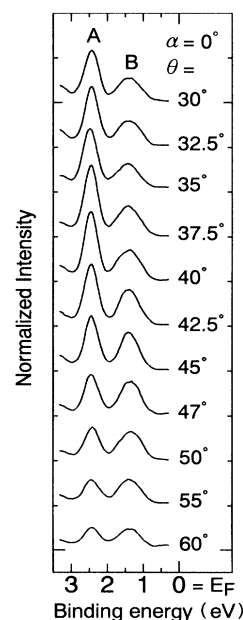


FIG. 2. The takeoff angle (θ) dependence of ARUPS spectra at incidence angle $\alpha=0^\circ$ and $h\nu=40$ eV in the binding-energy region of 0~3.5 eV. The intensity of the spectra is normalized to the incidence photon flux. The NHOMO and HOMO bands are indicated by *A* and *B*.

the HOMO band gives a maximum at $\theta_{\max} \simeq 45^\circ$; (2) the maximum intensity of NHOMO band is more intense than that of the HOMO band; and (3) the FWHM (full width at half maximum) of the HOMO band is much larger than that of the NHOMO band.

According to the IAC approximation by Grobman,¹⁹ the total amplitude A_{tot} of the photoelectron from the n th molecular orbital is represented by

$$A_{\text{tot}}(\mathbf{R}) = \frac{e^{ikR}}{R} \sum_a C_{na} e^{-ik \cdot \mathbf{R}_a} \sum_{l,m} M_{l,a}^m y_l^m(\hat{\mathbf{R}}). \quad (1)$$

The first term is the damping factor of spherical waves at the detector position \mathbf{R} ($=R\hat{\mathbf{R}}$). The sum over contribu-

tions from individual atoms a makes up A_{tot} . C_{na} is the atomic orbital coefficient of the n th molecular orbital. The term $e^{-ik \cdot \mathbf{R}_a}$ is the phase factor due to the difference in the path length to the detector from each atomic position \mathbf{R}_a , where \mathbf{k} ($=k\hat{\mathbf{R}}$) is the wave vector of the photoelectron. The term $\sum_{l,m} M_{l,a}^m y_l^m(\hat{\mathbf{R}})$ is the so-called atomic factor for optical excitation from an initial state to final continuum states. Goldberg, Fadley, and Kono²⁵ computed this value within the one-electron, central-potential model and dipole approximation for atomic orbitals of s , p_x , p_y , p_z , d_{xy} , d_{yz} , d_{xz} , d_{z^2} , and $d_{x^2-y^2}$, as previously discussed for d orbitals by Gadzuk.²⁶ Using their results, the atomic factor of p_z orbitals ($|l,m\rangle = |1,0\rangle$) in Eq. (1) becomes

$$M_{l,a}^m y_l^m(\hat{\mathbf{R}}) \propto \langle \phi_{E_{\text{kin},k}} | \hat{\mathbf{e}} \cdot \mathbf{r} | \phi_{nlm} \rangle \\ \equiv (-i)^{l-1} \{ \exp(i\delta_{l-1}^a) X_{l-1,m'}^a + \exp(i\delta_{l+1}^a) X_{l+1,m'}^a \}, \quad (2)$$

$$X_{l-1,m'}^a = 2(2\pi)^{1/2} R_s^a [(\frac{1}{6})^{1/2} \epsilon_z], \quad (3)$$

$$X_{l+1,m'}^a = 2(2\pi)^{1/2} R_d^a [(\frac{3}{2})^{1/2} \sin\theta_k \cos\theta_k (-\epsilon_x \cos\phi_k - \epsilon_y \sin\phi_k) - \epsilon_z (\frac{1}{6})^{1/2} (3 \cos^2\theta_k - 1)], \quad (4)$$

$$\epsilon_x = \sin\theta_\epsilon \cos\phi_\epsilon, \quad \epsilon_y = \sin\theta_\epsilon \sin\phi_\epsilon, \quad \epsilon_z = \cos\theta_\epsilon, \quad (5)$$

where $\phi_{E_{\text{kin},k}}$ is the final-state wave function of the kinetic energy E_{kin} and wave vector \mathbf{k} . ϕ_{nlm} is the initial-state wave function. $X_{l\pm 1,m'}^a$ are the components of the dipole matrix element. They are expressed by the partial wave components of final states allowed by the dipole selection rule ($\Delta l = l' - l = \pm 1$, $\Delta m = m' - m = \pm 1$ and 0), where R_s^a and R_d^a are the radial matrix elements for s ($\Delta l = -1$)- and d ($\Delta l = +1$)-type final states. $\delta_{l\pm 1}^a$ are the phase shifts of the partial waves, which include Coulombic and non-Coulombic effects of the total atomic potential.^{25,26} $\hat{\mathbf{e}} = (\epsilon_x, \epsilon_y, \epsilon_z)$ is the direction of the photon polarization. The angles θ_k, ϕ_k , and $\theta_\epsilon, \phi_\epsilon$ specify the photoemission direction and the polarization direction of the incidence photon, respectively.

Using Eqs. (1)–(5), we calculated the θ dependence of the photoelectron intensity from the NHOMO and HOMO states of an oriented BTQBT molecule. In the calculation, we introduced the inclination angle β at which the molecular plane is inclined to the substrate surface and the molecular azimuthal angle ϕ_m specifying the azimuthal orientation in the molecular plane, as shown in Fig. 3. HOPG exhibits azimuthal disorder due to micrograin structures. In fact, the HOPG substrate showed no clear azimuthal angle dependence on ARUPS spectra, since the incidence-beam size at the surface is larger than the grain size. Thus the calculation was carried out by averaging over the substrate azimuthal angle ϕ_s around the substrate normal \mathbf{n}_s (see Fig. 3). The values of atomic coefficient C_{na} were taken from the results of MNDO molecular-orbital calculations.²⁷ The atomic positions \mathbf{R}_a were obtained by x-ray structural analysis on the single crystal.¹⁶ For R_s^a , R_d^a , and $\delta_{l\pm 1}^a$ of carbon- $2p_z$ and sulfur- $3p_z$ orbitals, we used the values calculated by Goldberg, Fadley, and Kono of $h\nu = 40.8$

eV.²⁵ Since those values for the nitrogen- $2p_z$ orbital were not tabulated, we used the averages of the values for carbon- and oxygen- $2p_z$ orbitals. The final-state kinetic energies E_{kin} of the NHOMO and HOMO bands were experimentally determined to be 33.2 and 34.3 eV.²⁸ In the present calculation, we assumed the complete polarization of the incidence photon.

In organic solids, the intermolecular interaction is usually weak, since the molecules are condensed dominantly by weak van der Waals forces. On the other hand, a tight-binding band calculation showed that the HOMO band of BTQBT has an unusual large transfer integral, i.e., a strong intermolecular interaction,²⁹ and it causes a large bandwidth for the HOMO state, as observed in Fig. 2. In addition, we recently observed a clear energy-band dispersion for the HOMO band from the incidence pho-

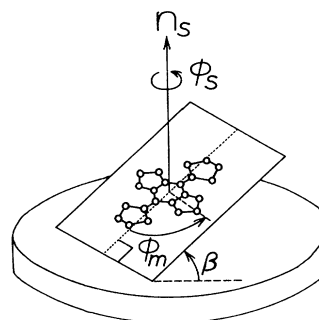


FIG. 3. Illustration of a BTQBT molecule with inclination angle β to the substrate. Molecular azimuthal angle ϕ_m is defined in the molecular plane. ϕ_s is the substrate azimuthal angle around the substrate normal \mathbf{n}_s .

ton energy ($h\nu$) dependence of the normal emission spectra, while the NHOMO band exhibited only a little dispersion.³⁰ This also confirms the existence of the strong intermolecular interaction for the HOMO state. Since the present method of analysis neglects such interaction and regards the molecule as an oriented gas, we first compare the calculated results with experimental ones for the NHOMO band.

In Figs. 4(a)–4(d), the calculated angular distributions of photoelectrons for the NHOMO state at inclination angles $\beta=0^\circ$, 5° , 10° , and 20° are shown, where the dotted, broken, and solid lines in each figure are the results at molecular azimuthal angles $\phi_m=0^\circ$, 30° , and 90° , respectively. The experimental results are also shown by open circles. They are normalized to the maximum intensity at θ_{\max} . At inclination angle $\beta=0^\circ$ (a), i.e., the case where the molecule lies perfectly flat on the substrate surface, the calculated distribution curve exhibits a maximum at an angle similar to the experimental result, while the curve shape near θ_{\max} is a little broader. In this case, the calculated result is independent of ϕ_m . At $\beta=5^\circ$ (b), the calculated curves are almost similar to the curve at $\beta=0^\circ$ (a). However, the curve shape at $\beta=5^\circ$ and $\phi_m=90^\circ$ becomes sharp, and gives the best fit with the experimental results for both the shape and direction of maximum intensity. At $\beta=10^\circ$ (c), the shape of each curve becomes broader than that at $\beta=5^\circ$ (b), and the ϕ_m dependence appears clearly. At $\beta=20^\circ$ (d), the ϕ_m dependence becomes more significant, and the disagreement between

the calculated and experimental results becomes apparent. Although the calculated distribution curve at $\beta=5^\circ$ and $\phi_m=90^\circ$ gives the best agreement with the experimental results, we expect that the BTQBT molecules lie with the inclination angle $\beta \leq 10^\circ$ to the HOPG surface by considering the experimental error and the neglect of various scattering effects in the calculation. In the single crystal,¹⁶ the BTQBT molecules form a sheetlike structure and each molecule orients at $\beta=5^\circ$ and $\phi_m=90^\circ$ (Fig. 1). These values are in good agreement with those obtained by the present comparison between the calculated and experimental results.

In Fig. 5, the calculated distribution curves and experimental results for the HOMO band at $\beta=5^\circ$ are shown. For comparison with the NHOMO band, the intensity scale is similar to that for the NHOMO band [Fig. 4(b)]. As seen in Fig. 5, an advantage of the present method of analysis is that the relative intensities of the different target bands (HOMO and NHOMO bands) are calculable. Although the calculated curve at $\phi_m=90^\circ$ agrees with the experimental results about the maximum intensity as well as shape of the curve, the angle for maximum intensity θ_{\max} is about 10° lower than the experimental results. The disagreement may be caused by the strong intermolecular interaction for HOMO states in the solid film, and further investigation of this point is in progress.

In the present case, the calculated spectra, considering only the molecule itself, showed fairly good agreement with the experimental results, though we used the present method as a first step of our analysis. This might be the result of (i) a large lattice mismatch between the substrate and the atoms constituting the large molecule which will effectively smear out the backscattering from the substrate,³¹ and (ii) the present measurement condition in which the perturbation of the scattering from neighboring molecules is expected to be small.³² Although it seems that the multiple-scattering effects did not contribute as much to the present takeoff angle dependence as expected for adsorbates on metal surfaces,³ they should be considered for much better agreement.

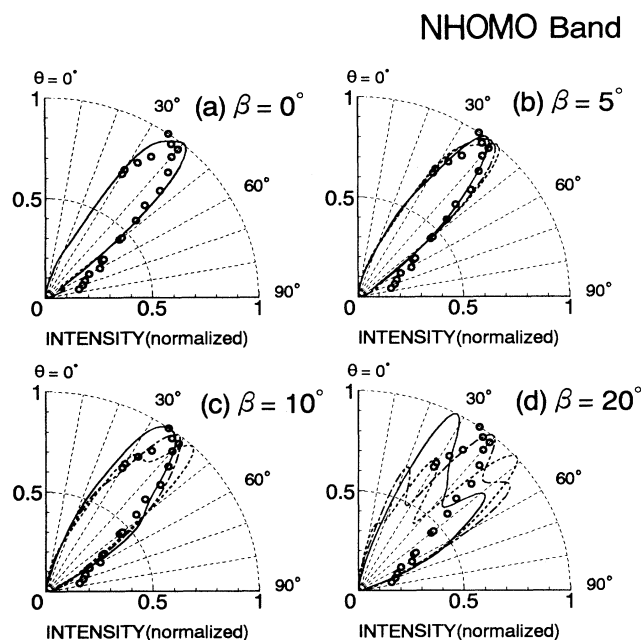


FIG. 4. The takeoff angle (θ) dependences of photoemission intensities for the NHOMO band at $\alpha=0^\circ$. The calculated angular distributions using inclination angles β =(a) 0° , (b) 5° , (c) 10° , and (d) 20° are shown. The dotted, broken, and solid lines in each figure are the results at $\phi_m=0^\circ$, 30° , and 90° , respectively. The experimental results are plotted by open circles in each figure.

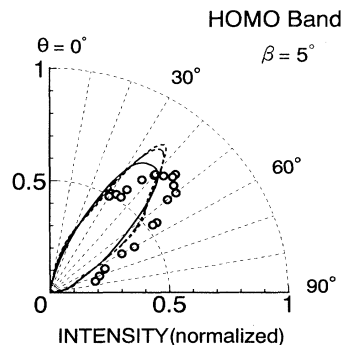


FIG. 5. The takeoff angle (θ) dependences for the HOMO band at $\alpha=0^\circ$. The inclination angle is $\beta=5^\circ$, where the intensity scale is the same as in Fig. 4(b). The dotted, broken, and solid lines in each figure are at $\phi_m=0^\circ$, 30° , and 90° , respectively. The experimental results are shown by open circles.

SUMMARY

We measured the takeoff angle (θ) dependence of the photoelectron intensity from the two highest bands of BTQBT thin films, and used the IAC approximation combined with the MNDO molecular-orbital calculation in the analysis. From the comparison between the calculated and experimental results, the BTQBT molecules in the thin film were estimated to lie within the inclination angle $\beta \leq 10^\circ$ to the HOPG substrate. The present method was also applied to ultrathin films of H_2 - and Cu-phthalocyanine, and a good agreement between calculated and experimental results was obtained.³¹

In this paper, we have demonstrated that the present method of analysis is a useful first step in directing the quantitative analyses of ARUPS for large and complex organic molecules. For a more complete analysis, it would be necessary to use exact values of R_s^a , R_d^a , and $\delta_{\pm 1}^a$ for various kinetic energies,²⁵ and to take account of the intermolecular interaction,²⁰ the surface barrier effect

by the inner potential,³³ and the scatterings of photoelectrons by neighboring atoms, molecules, and substrate.³⁻⁵ With improvement in these factors, ARUPS will become a more useful technique for characterizing the thin films of large organic systems.

ACKNOWLEDGMENTS

One of the authors (S.H.) wishes to thank Professor Y. Maruyama for his kind support. N.U. thanks Professor F. P. Netzer for fruitful discussions on the quantitative analysis of angle-resolved photoemission spectra. The authors thank Professor K. Nasu, Dr. T. Mori, Dr. K. Imaeda, and Mr. K. Suzuki for much helpful advice. The authors acknowledge the staff of the UVSOR facility in IMS for their considerate support. This work was supported by the Joint Studies Program (1991-1992) of the Institute for Molecular Science and by a Grant-in-Aid for Scientific Research on New Program (04NP0301) from the Ministry of Education, Science and Culture of Japan.

¹A. Liebsch, *Photoemission and the Electronic Properties of Surfaces*, edited by B. Feuerbacher, B. Fitton, and R. F. Willis (Wiley, New York, 1978), Chap. 7, and references therein.

²N. V. Richardson and A. M. Bradshaw, *Electron Spectroscopy*, edited by C. R. Brundle and A. D. Baker (Academic, New York, 1982), Vol. 4, Chap. 3, and references therein.

³A. Liebsch, *Phys. Rev. B* **13**, 544 (1976).

⁴K. Kambe and M. Scheffler, *Surf. Sci.* **89**, 262 (1979).

⁵D. Dill and J. L. Dehmer, *J. Chem. Phys.* **61**, 692 (1974).

⁶J. W. Davenport, *Phys. Rev. Lett.* **36**, 945 (1976).

⁷K. Horn, A. M. Bradshaw, and K. Jacobi, *Surf. Sci.* **72**, 719 (1978).

⁸F. P. Netzer, *Vacuum* **41**, 49 (1990).

⁹M. G. Ramsey, G. Rosina, F. P. Netzer, H. B. Saalfeld, and D. R. Lloyd, *Surf. Sci.* **218**, 317 (1989).

¹⁰P. Yannoulis, K. H. Frank, and E. E. Koch, *Surf. Sci.* **241**, 325 (1991).

¹¹P. Yannoulis, K. H. Frank, and E. E. Koch, *Surf. Sci.* **243**, 58 (1991).

¹²T. Permien, R. Engelhardt, C. A. Feldmann, and E. E. Koch, *Chem. Phys. Lett.* **98**, 527 (1983).

¹³N. V. Richardson, *Chem. Phys. Lett.* **102**, 390 (1983).

¹⁴G. L. Nyberg and N. V. Richardson, *Surf. Sci.* **85**, 335 (1979).

¹⁵B. J. Bandy, D. R. Lloyd, and N. V. Richardson, *Surf. Sci.* **89**, 344 (1979).

¹⁶Y. Yamashita, S. Tanaka, K. Imaeda, and H. Inokuchi, *Chem. Lett.* **7**, 1213 (1991).

¹⁷K. Imaeda, Y. Yamashita, Y. Li, T. Mori, H. Inokuchi, and M. Sano, *J. Mater. Chem.* **2**, 115 (1992).

¹⁸H. Inokuchi, K. Imaeda, T. Enoki, T. Mori, Y. Maruyama, G. Saito, N. Okada, H. Yamochoi, K. Seki, Y. Higuchi, and N. Yasuoka, *Nature* **329**, 39 (1987).

¹⁹W. D. Grobman, *Phys. Rev. B* **17**, 4573 (1978). We believe that the phase factor $e^{ik \cdot R^a}$ in Eq. (2.17) in this paper should read $e^{-ik \cdot R^a}$.

²⁰N. J. Shevchik, *J. Phys. C* **11**, 3521 (1978).

²¹J. J. P. Stewart, *Q.C.P.E. Bull.* **3**, 43 (1983).

²²N. Ueno, K. Seki, N. Sato, H. Fujimoto, T. Kuramochi, K. Sugita, and H. Inokuchi, *Phys. Rev. B* **41**, 1176 (1990).

²³K. Seki, H. Nakagawa, K. Fukui, E. Ishiguro, R. Kato, T. Mori, K. Sakai, and M. Watanabe, *Nucl. Instrum. Methods A* **246**, 264 (1986).

²⁴H. Fujimoto, K. Kamiya, S. Tanaka, T. Mori, Y. Yamashita, H. Inokuchi, and K. Seki, *Chem. Phys.* **165**, 135 (1992).

²⁵S. M. Goldberg, C. S. Fadley, and S. Kono, *J. Electron Spectrosc. Relat. Phenom.* **21**, 285 (1981).

²⁶J. W. Gadzuk, *Phys. Rev. B* **12**, 5608 (1975).

²⁷S. Tanaka *et al.* (unpublished).

²⁸In the present calculation, we demonstrate the results for the inner potential $V_0=0$ eV. Our preliminary calculation considering the V_0 effect (Ref. 33) gave almost the same results as $V_0=0$ eV, since the refraction of photoelectrons due to the inner potential was compensated for by a change of interference effect.

²⁹T. Mori *et al.* (unpublished).

³⁰S. Hasegawa *et al.* (unpublished).

³¹N. Ueno *et al.* (unpublished).

³²For example, Kambe and Scheffler calculated the takeoff angle dependence for oxygen adsorbed on a Ni surface using the Green functions of atomic, adlayer, and substrate parts (Ref. 4). For the emission from the oxygen $2p_z$ state at $\alpha=0^\circ$ and $h\nu=40.8$ eV, corresponding to the present condition, the calculated spectrum considering multiple scattering in the oxygen layer is almost the same as that from the atomic part. The scattering from the substrate will be effectively weakened in the present case, since the film thickness was thicker than the photoelectron escape depth.

³³M. Scheffler, K. Kambe, and F. Forstmann, *Solid State Commun.* **25**, 93 (1978).